RAPID COMMUNICATIONS

PHYSICAL REVIEW B VOLUME 48, NUMBER 2 1 JULY 1993-II

Observation of a disordered vortex state in $Bi_2Sr_2CaCu_2O_{8+x}$ single crystals containing columnar defects

M. Leghissa, L. A. Gurevich,* M. Kraus, and G. Saemann-Ischenko
Physikalisches Institut, Universität Erlangen-Nürnberg, Erwin-Rommel-Strasse 1, D-91058 Erlangen, Germany

L. Ya. Vinnikov
Institute of Solid State Physics, Chernogolovka, Moscow Distict, 142432, Russia
(Received 30 April 1993)

We report on the visualization of vortex patterns by means of the high-resolution Bitter-decoration technique in $Bi_2Sr_2CaCu_2O_{8+x}$ single crystals containing columnar defects generated via high-energy heavy-ion irradiation. By irradiating only a part of each sample, a simultaneous decoration of irradiated and nonirradiated parts was possible. The columnar defects lead to a complete destruction of translational order, whereas the vortex lattice in the nonirradiated parts exhibits hexagonal ordering. Analyses of the decoration images yield translational correlation lengths of 1.5 to 2 flux spacings in the nonirradiated areas and about 0.5 flux spacings in the irradiated areas.

The observation of flux lattices using the high-resolution Bitter-pattern technique provides a method to investigate the microscopic response of the vortex system to the forces acting due to vortex-vortex interaction as well as the interactions with pinning centers, i.e., crystal-lattice defects introducing disorder and the intrinsic layered structure of the high-T_c superconductors. A number of vortex structures have been found to exist due to the specific properties of the high-T_c compounds, e.g., the hexatic vortex glass,[1] vortex chains for magnetic fields tilted with respect to the c axis,[2,3] anisotropic vortex structures,[4] and oval vortices for the magnetic field aligned parallel to the a-b plane.[5]

Extended (linear and planar) defects appear to be the most effective pinning centers for flux lines. These defects can be either due to the sample preparation procedure (e.g., twin boundaries and dislocations) or artificially generated columnar defects introduced through high-energy heavy-ion irradiation. In several papers the pinning of vortices by twin boundaries has been confirmed by means of magnetic decoration.[6–8] However, the effects of columnar defects have only been investigated using the macroscopic magnetization[9,10] and transport current methods,[11,12] and by the high-resolution Faraday technique,[13,14] which yields local information about the flux density without being able to resolve single vortices.

In this paper we report the direct observation of vortices in $Bi_2Sr_2CaCu_2O_{8+x}$ single crystals containing columnar defects due to irradiation with 340-MeV Xe ions. We will show simultaneous decoration of irradiated and nonirradiated regions. The basic result of our Bitter patterns is a highly disordered vortex state due to pinning by the columnar defects, whereas the nonirradiated parts show a hexagonally correlated flux lattice.

The $Bi_2Sr_2CaCu_2O_{8+x}$ single crystals were grown from the melt using Al_2O_3 crucibles. Typical dimensions of our samples were $1 \times 2 \times 0.05$ mm^3 with the smallest direction being along the c axis. Measurements of critical current densities and activation energies by means of magnetization measurements and magneto-optical investigations, both before and after heavy-ion irradiation, have been published elsewhere.[10,13,14]

In Fig. 1 the basic setup for the irradiation procedure is sketched. The irradiation with 340-MeV Xe ions parallel to the c axis was performed at the VICKSI facility of the Hahn-Meitner-Institut (Berlin). Fluences of $\phi t = 5.9 \times 10^9$, 1.2×10^{10}, and 1.7×10^{10} ions/cm^2 were used. To compare the defect density with the vortex density it is useful to introduce the so-called dose-equivalent field $B_{\phi t} = \Phi_0 \phi t$, where Φ_0 is the flux quantum. The corresponding dose-equivalent fields are $B_{\phi t} = 1.2$, 2.5, and 3.5 kG, respectively. In order to perform simultaneous decoration on irradiated and nonirradiated parts of one sample, each crystal was partly covered with an Cu absorber plate during the ion bombardment. The projected range of the 340-MeV Xe ions is 21 μm, and the depth to which the columnar defects extend is about 9 μm, based on a threshold of $S_e = 2$ keV/Å for the electronic energy

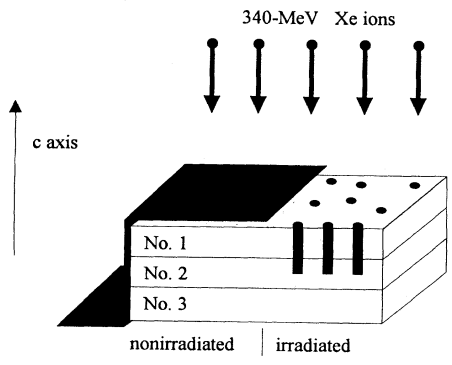

FIG. 1. Schematic setup of the irradiation experiments.

loss. After 21 μm the projectile ions are implanted within the crystals, leaving the lower part of the samples unaffected by irradiation. Therefore each crystal consists of three different types of "samples" labeled as No. 1, No. 2, and No. 3: the surface sheet (No. 1) containing continuous columnar defects, the middle sheet (No. 2) containing the part where the projectiles are stopped, and finally the bottom sheet (No. 3) which is not modified due to irradiation. From high-resolution TEM investigations on $Bi_2Sr_2CaCu_2O_{8+x}$ thin films an average track diameter of 70 Å has been determined.

Freshly cleaved samples were field cooled from room temperature down to 4.2 K with the magnetic field applied parallel to the c axis and hence also parallel to the columnar defects. At a certain (in principle unknown) temperature T_f the vortex arrangement is frozen due to the increasing activation energies and the decreasing thermal fluctuations. Then the trapped flux lines were imaged using the high-resolution Bitter technique by decorating the surface of the samples with fine Fe particles.[6] Figures 2 and 3 show patterns obtained on the bottom surface of sheet No. 1 (see Fig. 1) at a magnetic field of 22 G for the crystal irradiated at the highest fluence ($B_{\phi t}$ = 3.5 kG). Since $B_{\phi t}$ is always much larger than the applied field $B_{\rm ext}$ we did not observe any significant fluence dependence of the patterns. Figure 2 corresponds to the nonirradiated half and Fig. 3 to the irradiated one. In Fig. 2 a hexagonal vortex lattice extending over several vortex spacings $a_0 = \sqrt{\Phi_0/B}$ is clearly visible. This confirms the good quality of the as-grown crystals. Completely different patterns are observed in the irradiated region, as shown in Fig. 3. The positions of the vortices are uncorrelated and no hexagonal ordering is visible. In order to confirm that this effect is due to the irradiation

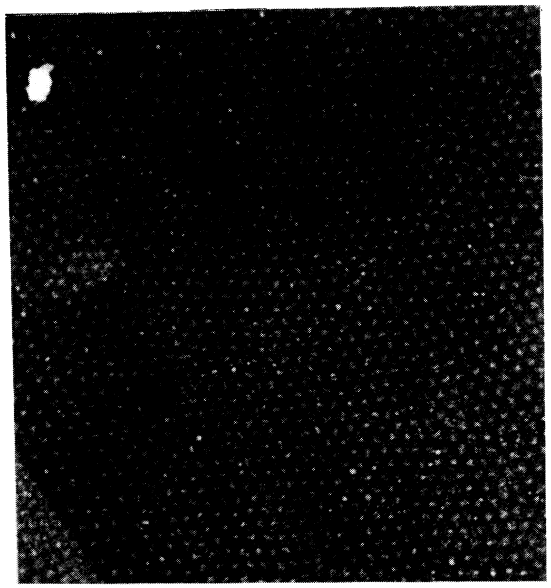

FIG. 2. Bitter pattern for a nonirradiated region. A magnetic field of 22 G is applied parallel to the c axis.

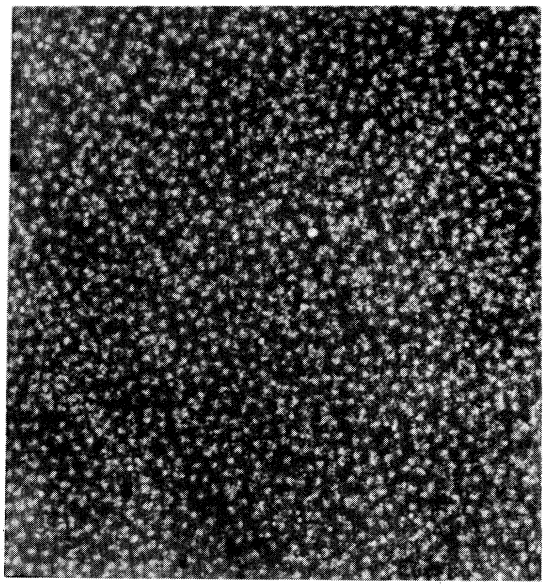

FIG. 3. Bitter pattern for a region with columnar defects. Field and scale as in Fig. 2.

induced defects, decoration patterns have been recorded on the top surface of sheet No. 3. This sheet belongs to the lower part of the sample below the penetration depth of the projectile ions. Patterns observed on this surface always looked like the vortex lattice shown in Fig. 2.

A quantitative analysis of the vortex patterns can be performed by calculating the radial correlation functions of the images defined as

$$G(r) \propto \int\int I(\mathbf{r}')I(\mathbf{r}'-\mathbf{r})d^2\mathbf{r}'\,d\varphi, \qquad (1)$$

which is a measure for the translational order of the patterns. Here $I(\mathbf{r}')$ is the intensity at $\mathbf{r}'$ and φ is the azimuth angle. In Fig. 4 plots of $G(r)$ both in the irradiated and nonirradiated region are shown. As indicated in the decoration images, the vortex patterns in the as-grown crystals exhibit at least short-range translational ordering and several peaks at na_0 (up to $n = 3$) are clearly visible. For the irradiated parts only the nearest neighbor ($n = 1$) yields a significant maximum in the correlation function. The translational correlation length R_c has been determined by a fit to $G(r) = G_0(r)\exp(-r/R_c)$ with $G_0(r)$ denoting the correlation function of the undisturbed triangular lattice.[15] The fits are shown in Fig. 4 as lines and yield values for the correlation length of $R_c \approx 1.5a_0$ to $2a_0$ for the nonirradiated parts and $R_c \approx 0.5a_0$ for the parts with columnar defects, respectively.

The above described results suggest that each vortex is individually pinned by a columnar defect, resulting in an extremely short correlation length of $R_c \approx 0.5a_0$. Since $B_{\phi t}$ is about two orders of magnitude larger than the applied magnetic field, the defect density clearly outnumbers the typical vortex density. Recently it has

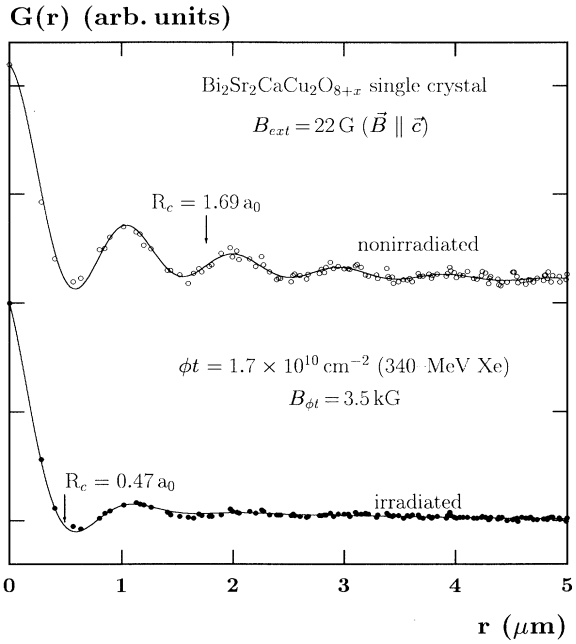

FIG. 4. Shown are the radial correlation functions $G(r)$ both in the irradiated (closed circles) and nonirradiated parts (open circles) for a $Bi_2Sr_2CaCu_2O_{8+x}$ single crystal. Estimates of the translational correlation length R_c are labeled by arrows.

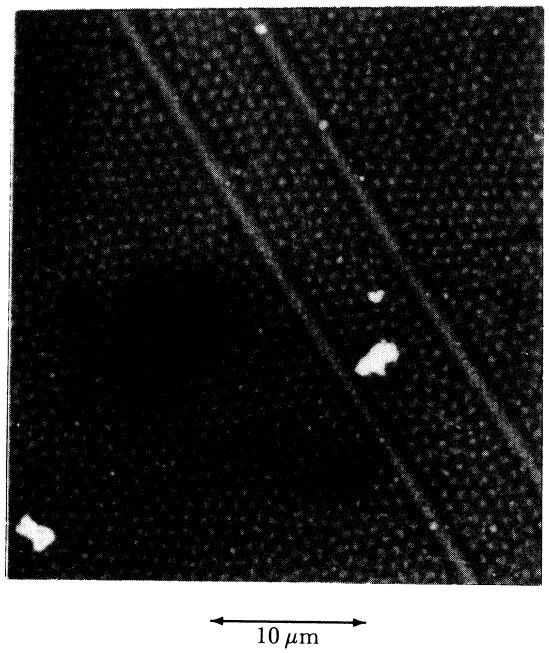

FIG. 5. Vortex pinning by extended preparation-induced defects. Due to the reduced vortex spacing the flux lines inside the chain cannot be resolved.

been shown that columnar defects lead to a considerable shift of the irreversibility line in $Bi_2Sr_2CaCu_2O_{8+x}$.[16,17] Therefore they provide relatively strong pinning centers even at high temperatures. Upon cooling the vortices will adjust to the randomly distributed ion tracks. Since every vortex easily finds a defect, this situation corresponds to the regime of single vortex pinning and a random distribution of flux lines is obtained. Therefore the translational order in the irradiated parts is highly suppressed. For the nonirradiated parts the picture of collective pinning applies, resulting in a disordered hexagonal vortex lattice with a correlation radius between 1.5 and 2 flux spacings. The high degree of disorder in the irradiated region may also be a hint for a higher freezing temperature T_f compared to the nonirradiated parts.

Additionally to the disorder generated by the columnar defects we observe also vortex pinning by extended preparation-induced defects. In Fig. 5 a Bitter pattern on the surface of a nonirradiated region is shown. Besides the hexagonal vortex lattice we observe straight lines with an extreme small vortex spacing. In fact we have not been able to resolve single vortices along these lines. We find these chains mainly in the nonirradiated parts with an average density of 0.1 μm^{-1}, indicating that columnar tracks act as more efficient pinning centers than these defects. The vortex lattice nearby is aligned in parallel to these line defects. However, between the lines and the lattice there is a vortex-free belt of about 2 flux lattice constants, presumably due to the repulsion caused by the enhanced vortex density along the lines. Similar patterns have been reported by Bishop *et al.* for $Bi_2Sr_2CaCu_2O_{8+x}$ (Ref. 15) and by Grigorieva *et al.* for Al-doped $YBa_2Cu_3O_{7-\delta}$.[18] In Ref. 18 a correlation of these lines with growth steps and surface undulations has been found. It is presently unclear whether our observations correspond to the results of Ref. 18 obtained on $YBa_2Cu_3O_{7-\delta}$ crystals, or whether these structures are caused by stacking faults and/or dislocations.

In conclusion, we have investigated the influence of columnar defects on the vortex pattern of $Bi_2Sr_2CaCu_2O_{8+x}$ single crystals. Simultaneous decoration of irradiated and nonirradiated parts as well as depth sensitive studies clearly demonstrate the huge effects caused by columnar defects. In the limit of high defect densities ($B_{\phi t} \gg B_{\rm ext}$) a completely disordered vortex state indicates strong pinning of single vortices by the ion tracks. From the radial correlation function a translational correlation length of $R_c \approx 0.5 a_0$ has been found in the irradiated parts. This finding confirms that vortices are individually pinned by the columnar defects. In addition, preparation-induced extended defects have been found to result in chains with a reduced vortex spacing.

We thank S. Klaumünzer (HMI Berlin), P. Bauer, and D. Nagengast (University of Erlangen) for helpful assistance and discussion. One of us (L.A.G.) wants to thank the DAAD for financial support. This work was supported by the Bayerische Forschungsstiftung Hochtemperatur-Supraleitung (FORSUPRA) and the Bundesministerium für Forschung und Technologie.

*Permanent address: Institute of Solid State Physics, Chernogolovka, Russia.

[1]D.J. Bishop, P.L. Gammel, D.A. Huse, and D.A. Murray, Nature (London) **255**, 165 (1992).

[2]C.A. Bolle, P.L. Gammel, D.G. Grier, C.A. Murray, D.J. Bishop, D.B. Mitzi, and A. Kapitulnik, Phys. Rev. Lett. **66**, 112 (1991).

[3]P.L. Gammel, D.J. Bishop, J.P. Rice, and D.M. Ginsberg, Phys. Rev. Lett. **68**, 2243 (1992).

[4]L.Ya. Vinnikov, I.V. Grigorieva, L.A. Gurevich, and Yu.A. Ossipyan, Pis'ma Zh. Eksp. Teor. Fiz. **49**, 83 (1989) [Sov. Phys. JETP Lett. **49**, 99 (1989)].

[5]G.J. Dolan, F. Holtzberg, C. Feild, and T.R. Dinger, Phys. Rev. Lett. **62**, 2184 (1989).

[6]L.Ya. Vinnikov, L.A. Gurevich, G.A. Yemelchenko, and Yu.A. Ossipyan, Solid State Commun. **67**, 421 (1988).

[7]I.V. Grigorieva, L.A. Gurevich, and L.Ya. Vinnikov, Physica C (Amsterdam) **195**, 327 (1992).

[8]P.L. Gammel, C.A. Durán, D.J. Bishop, V.K. Kogan, M. Ledvij, A.Yu. Simonov, J.P. Rice, and D.M. Ginsberg, Phys. Rev. Lett. **69**, 3808 (1992).

[9]L. Civale, A.D. Marwick, T.K. Worthington, M.A. Kirk, J.R. Thompson, L. Krusin-Elbaum, Y. Sun, J.R. Clem, and F. Holtzberg, Phys. Rev. Lett. **67**, 648 (1991).

[10]W. Gerhäuser, G. Ries, H.W. Neumüller, W. Schmidt, O. Eibl, G. Saemann-Ischenko, and S. Klaumünzer, Phys. Rev. Lett. **68**, 879 (1992).

[11]B. Roas, B. Hensel, S. Henke, S. Klaumünzer, B. Kabius, W. Watanabe, G. Saemann-Ischenko, L. Schultz, and K. Urban, Europhys. Lett. **11**, 669 (1990).

[12]R.C. Budhani, M. Suenaga, and S.H. Liou, Phys. Rev. Lett. **69**, 3816 (1992).

[13]M. Leghissa, Th. Schuster, W. Gerhäuser, S. Klaumünzer, M.R. Koblischka, H. Kronmüller, H. Kuhn, H.-W. Neumüller, and G. Saemann-Ischenko, Europhys. Lett. **19**, 323 (1992).

[14]Th. Schuster, M. Leghissa, M.R. Koblischka, H. Kuhn, M. Kraus, H. Kronmüller, and G. Saemann-Ischenko, Physica C (Amsterdam) **203**, 203 (1992).

[15]D.J. Bishop, P.L. Gammel, C.A. Murray, D.B. Mitzi, and A. Kapitulnik, Physica C (Amsterdam) **169**, 72 (1991).

[16]J.R. Thompson, Y.R. Sun, H.R. Kerchner, D.K. Christen, B.C. Sales, B.C. Chakoumakos, A.D. Marwick, L. Civale, and J.O. Thomson, Appl. Phys. Lett. **60**, 2306 (1992).

[17]V. Hardy, Ch. Simon, J. Provost, and D. Groult, Physica C (Amsterdam) **205**, 371 (1993).

[18]I.V. Grigorieva, K.E. Bagnall, P.A. Midgley, K. Sasaki, and J.W. Steeds, Physica C (Amsterdam) **199**, 73 (1992).

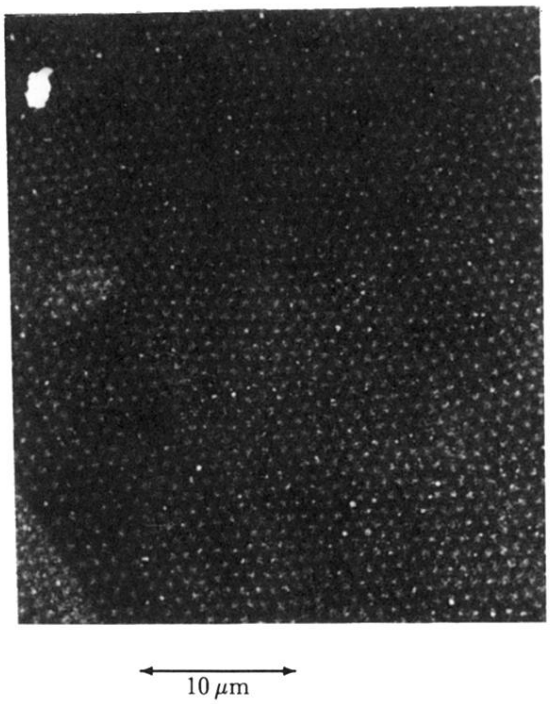

FIG. 2. Bitter pattern for a nonirradiated region. A magnetic field of 22 G is applied parallel to the c axis.

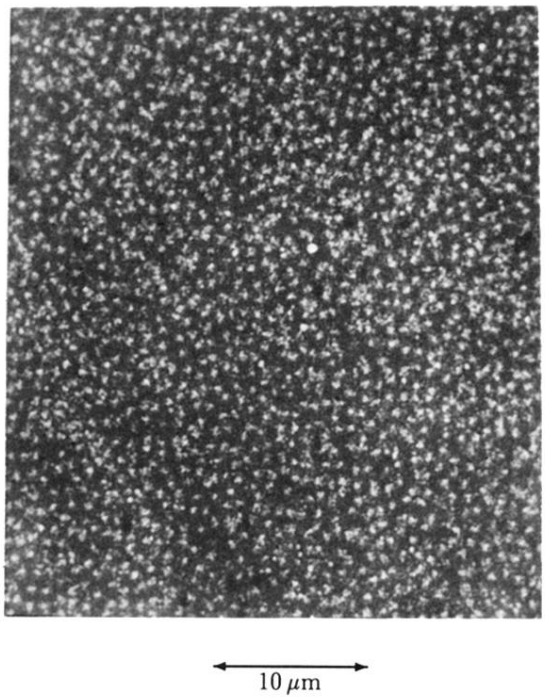

FIG. 3. Bitter pattern for a region with columnar defects. Field and scale as in Fig. 2.

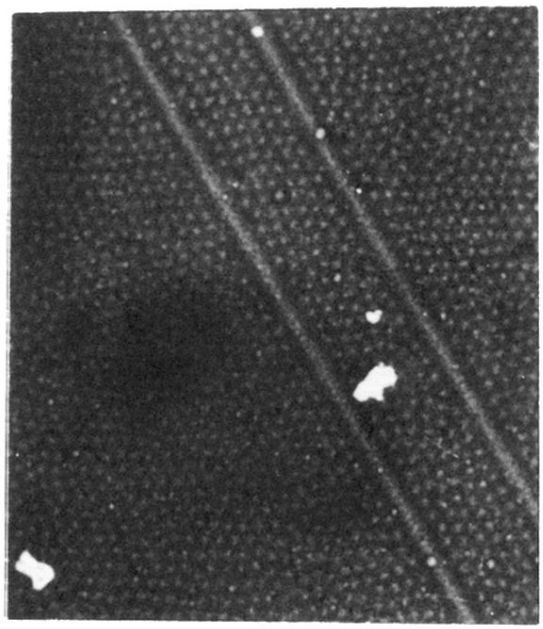

FIG. 5. Vortex pinning by extended preparation-induced defects. Due to the reduced vortex spacing the flux lines inside the chain cannot be resolved.